Photoelectron Spectra for a Two-Electron System in a Strong Laser Field

R. Grobe and J. H. Eberly

Department of Physics and Astronomy, University of Rochester, Rochester, New York 14627

(Received 26 August 1991; revised manuscript received 26 December 1991)

The strong-field behavior of a three-body quantum system analogous to a negative ion has been investigated by solving Schrödinger's equation nonperturbatively for two electrons on a two-dimensional lattice. Both photodetachment and core ionization have been studied, and we find that photospectral time dependence distinguishes between direct and stepwise ionization routes for the inner electron.

PACS numbers: 32.80.Rm

Strongly perturbed three-body systems inhabit a relatively unexplored domain in theoretical physics, and present a wealth of unsolved problems. In the area of atomic physics, the fundamental three-body systems are neutral helium (and its isoelectronic analogs), the atomic hydrogen negative ion, and the molecular hydrogen positive ion. Spectroscopic data for these systems are numerous regarding low-lying states, but information about high-lying states relating to the behavior of these systems under strong perturbations is almost completely absent. The main objective of this paper is to report new theoretical findings regarding two-electron ionization in a strong, pulsed laser field of optical or higher frequency.

By way of background it is important to know that in the last few years significant advances have been made in understanding the response of single-electron atoms to strong and superstrong radiation fields [1]. By the term strong field we will mean irradiation by a near-optical laser whose electric-field strength is $\mathcal{E} \approx 0.3$ a.u. or greater (intensity above 10^{15} W/cm^2). Related earlier work has included the experimental discovery of new single-electron phenomena such as above-threshold ionization (ATI) [2] and very-high-order harmonic generation [3], as well as theoretical predictions of stabilization of one-electron atoms under strong and superstrong fields [4].

In this paper we report energy levels and nonperturbative calculations of photoelectron spectra for a two-electron system. We have used the same strong-field lattice theory model with an infinitely heavy nucleus as Pindzola, Griffin, and Bottcher [5], but we have chosen the nuclear charge +1 instead of +2. Therefore our system can be tentatively identified as a one-dimensional analog of the hydrogen negative ion. For the static interaction between any two of the three particles, located at positions x_a and x_b, we use the soft-core Coulombic potential $V(x_a - x_b) = \pm [1 + (x_a - x_b)^2]^{-1/2}$ with the sign determined by the charges. The most prominent two-body properties of this potential are by now well known [6], but in a two-electron context its characteristics have not previously been explored, and we begin by reporting some spectral data (which we round off to two significant figures in dimensionless atomic units for simplicity throughout).

First, and most important, we have found that this system has only one bound state, as is the case for the real H^- ion. The single bound state is located at $E_g \approx -0.73$. There is a well-defined set of discrete energies above the detachment threshold that are associated with the bound states of the neutral atom and correspond to various (one-electron) thresholds. The energies of these states are already known [6] to be $E_n \approx -0.67$, -0.27, -0.15, -0.06, ..., and for high n we have Rydberg behavior: $E_n \approx -1/n^2$. Second, we can easily compute the ratio of the energies $E_1/E_g \approx 0.92$, which is the same (to within 5%) as for the real H/H^- ground-state energy ratio. Since this ratio is a rough measure of the importance of the e-e correlations in the atom, we have tentatively concluded that e-e correlations are not unduly distorted by the 1D aspects of our model. In addition, strong electron correlation effects are already evident in the ground-state wave function, which is shown in Fig. 1, along with a diagram based on the exact two-electron eigenenergies and showing the lowest thresholds.

To obtain the data just quoted we have solved numerically [7] the time-independent Schrödinger equation in the absence of any laser field. The eigenenergies are determined by the Hamiltonian

$$H_0 = \tfrac{1}{2} p_1^2 + \tfrac{1}{2} p_2^2 + V(x_1) + V(x_2) - V(x_1 - x_2), \qquad (1)$$

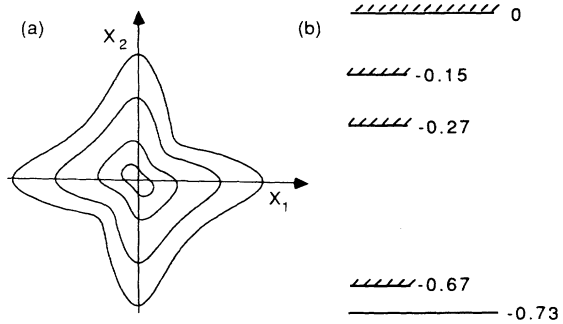

FIG. 1. (a) Contour plots of the probability density for the two-electron ground state. The fluted nature of the contours shows (i) that there is an "inner" and an "outer" electron, and (ii) that e-e repulsion along $x_1 = x_2$ is more pronounced than in Ref. [5], as expected. (b) An energy-level diagram based on the total two-electron energies. We display only the low-lying (one-electron) thresholds and the two-electron threshold, which we highlight by crosshatching.

where the potential $V(x)$ has been specified above. We have restricted our analysis to spin singlet states which are fully symmetric under the exchange of the electrons' spatial coordinates. As in the case of our previous single-electron calculations [6], and in common with Ref. [5], we have solved Eq. (1) above [and Eq. (2) below] directly, i.e., on a spatial lattice. The ground-state wave function was computed by starting with a Gaussian wave packet and then integrating Schrödinger's equation in imaginary time.

The behavior of two-electron atoms in laser fields is an interesting topic at any laser field strength, and the specific question of direct versus stepwise electron removal pathways in double ionization has been treated by weak-field perturbation theory and rate equations by a number of authors [8]. Some data are available from experiments [9] on alkaline-earth atoms and negative ions at low fields, including variable-frequency spectroscopy and observations of field-induced threshold shifts. Multiple-electron ionization in strong fields has been observed in several laboratories [10], but little about electron behavior [11] has been reported.

In the second stage of our calculations we introduced a laser field, and the two-electron system was allowed to interact with it in dipole approximation. The relevant time-dependent Schrödinger equation is then

$$i\partial\Psi(x_1,x_2,t)/\partial t=[H_0+(x_1+x_2)\mathcal{E}(t)\sin\omega t]\Psi(x_1,x_2,t)\,, \tag{2}$$

where $\mathcal{E}(t)$ denotes the temporal laser-pulse shape and ω the laser frequency. We prepared the electrons initially in the ground state. The total pulse duration was typically in the range 40–60 optical cycles, and the laser field amplitude $\mathcal{E}(t)$ was linearly turned on and off over two optical cycles [12]. In the field-strength range considered (see below) the lifetime of the ground state is shorter than 10 optical cycles, so we can expect most of the physics to be very well developed by the end of 40 cycles.

We now report our time-dependent results, which we present as photoelectron energy spectra. They show a number of interesting features, including spectral structure, different ionization rates for different channels, and several independent ATI series.

In order to calculate the electron energies following the laser pulse, the ground-state contribution was removed from the final wave function and the remainder $\psi(x_1,x_2,T)$ was Fourier decomposed into its momentum amplitude $\phi(k_1,k_2)$,

$$\phi(k_1,k_2)=\int\int dx_1\,dx_2\exp[i(k_1x_1+k_2x_2)]\times\psi(x_1,x_2,T)\,, \tag{3}$$

where k_1 and k_2 denote the momenta. An effective one-electron energy density $P(E)$ can be defined as the integral of $|\phi(k_1,k_2)|^2$ over one of the momenta, say k_2, and a subsequent transformation to energy via $E\equiv k_1^2/2$:

$$P(E)\equiv(2E)^{-1/2}\int dk_2|\phi(k_1,k_2)|^2\,. \tag{4}$$

The ranges of both laser frequency and field strength that are available for study are too wide to cover in any compact display. We show below only our results from the high-frequency and strong-field regime that has been of recent interest. We will present results for lower laser field strengths and frequencies elsewhere.

In Fig. 2(b) the low-energy photoelectron spectrum $P(E)$ is presented for $\mathcal{E}=0.5$ and $\omega=1$ (here ω was deliberately chosen to be large enough to exceed the two-electron threshold). We believe that these are the first calculations to produce a two-electron photospectrum using nonperturbative methods. Let us begin the interpretation of our results by viewing H^- as an ordinary hydrogen atom that is slightly modified by carrying an extra weakly bound electron. If we adopt such an extreme independent-electron view, as in Fig. 2(a), the weakly bound outer electron has its binding energy given by the photodetachment threshold energy, $E=-0.06$, while the inner electron has the binding energy of the core ground state, $E=-0.67$. This simplistic picture predicts that photopeaks can arise either from the ionization of the outer electron or of the inner electron (following channels A and B in the figure). These photopeaks should appear at the energies indicated in Fig. 2(a), and as Fig. 2(b) shows they do occur and $A1$ and $B1$ are the strongest peaks. In addition, the sum of their kinetic energies is $0.94+0.33=1.27$, and this equals $E_g+2\omega=-0.73+2$, as it should.

In other words, peaks $A1$ and $B1$, taken together, could be interpreted as a simultaneous two-photon double-ionization process. Whether this is appropriate or whether the two-electron process is stepwise cannot be answered by inspecting the long-time photospectrum.

However, one of the advantages of our method is that it allows the wave functions we have computed to be time resolved as well as energy resolved. We now show that time resolution allows one to see unambiguously that only

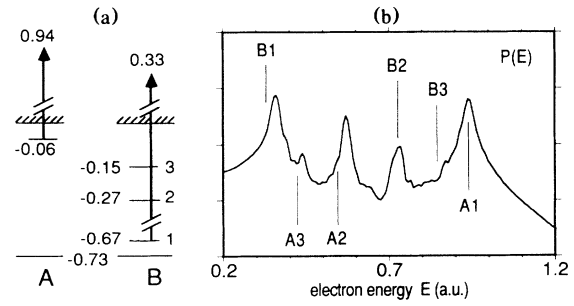

FIG. 2. (a) An energy-level diagram showing approximate independent-electron ionization channels for the weakly bound "outer" and strongly bound "inner" electron. (b) The one-electron photospectrum $P(E)$ for the laser pulse described in the text. The transition leading to the energies of peaks $A1$ and $B1$ are indicated by the arrows in (a), and the smaller peaks have energies corresponding to rearrangements within the core.

one interpretation of peaks $A1$ and $B1$ can be supported. Let us write two possible stepwise routes to the same final doubly ionized state as follows (the notation follows Fig. 2):

$$|g\rangle+\omega\rightarrow|E_{A1};n=1\rangle,\quad|E_{A1};n=1\rangle+\omega\rightarrow|E_{A1};E_{B1}\rangle, \tag{5}$$

$$|g\rangle+\omega\rightarrow|n^*;E_{B1}\rangle,\quad|n^*;E_{B1}\rangle+\omega\rightarrow|E_{A1};E_{B1}\rangle. \tag{6}$$

In both routes (5) and (6) there is a discrete intermediate state. In route (5) the outer electron is immediately detached while the inner electron "waits" in the core ground state $n=1$. In route (6) the outer electron "waits" in a high-lying Rydberg state n^* (there is accidentally a Rydberg state very conveniently located in this model at nearly exactly the detachment energy -0.06) while the inner electron is ejected immediately. The primary evidence is shown in Fig. 3(a) where snapshots are displayed of the photoelectron spectrum for 20-, 40-, and 60-cycle pulses. They indicate that the A peaks grow on a different time scale (more rapidly) than the B peaks.

The behavior in Fig. 3 can be compared with an analysis similar to that of Crance and Aymar [8]. From rate equations describing first route (5) and then route (6) one can compute the ratio of the population in the $B1$ peak to the population in the $A1$ peak. The corresponding predictions are shown against the computed data in Fig. 3(b), clearly favoring a definite time ordering that is

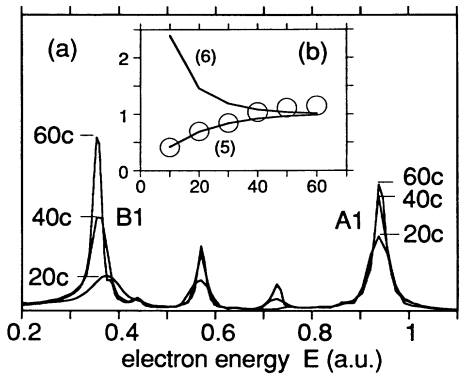

FIG. 3. The same one-electron spectrum $P(E)$ shown in Fig. 2(b), but for three different laser pulse durations: $T=20$, 40, and 60 cycles. Channel A peaks are prompt, initially growing rapidly, whereas channel B peaks start more slowly and are still growing rapidly between 40 and 60 cycles. Inset: The predictions of rate equations appropriate to routes (5) and (6). In both cases the transition rate coefficients were taken to be equal to the observed exponential ground-state decay rate. The time dependence of the ratio of the areas of peaks $B1$ and $A1$ in the numerical photoelectron spectra is indicated by circles. Route (5) is clearly preferred.

equivalent to stepwise ejection of the inner electron, and route (6) can be ruled out. On this basis it is clear that the satellite peaks $A2$, $A3$, etc., are one-photon two-electron shake-up peaks. That is, they arise from the detachment of the outer electron by one photon accompanied by shake-up of the inner electron into an excited core state. Satellite B peaks arise from subsequent ionization from these core excited states.

So far we have restricted our discussion to photopeak energies comparable to or smaller than the laser photon energy. However, single-electron atoms are well known to produce a discrete series of positive-energy (ATI) peaks accompanying ionization under a relatively strong laser field, as employed here. Various kinds of ATI series are conceivable in multiple-electron atoms and a number of them have been identified in an experimental study by Johann *et al.* [11]. As Fig. 4 shows, our wave functions predict ATI series of several types. For example, peak $A1$ [already shown in Fig. 2(b)] is the $s=0$ ATI peak associated with ionization (detachment in this case) of the first electron from the two-electron ground state, leaving the ionic core (atomic core in this case) in its lowest state. Figure 4 shows this peak and its corresponding $s=1$ and 2 peaks. Similarly, peak $B1$ of Fig. 2(b) is the $s=0$ peak associated with ionization of the second electron, and Fig. 4 shows it and the $s=1$ and 2 peaks in the corresponding ATI series. It is easy to see that not just $A1$ and $B1$ have associated series, but essentially all of the other peaks in Fig. 2(b) as well.

Let us summarize our results. We have presented in this Letter the results of strong-field lattice theory calculations on a two-electron atomic system. We have reported both bare energies and photoelectron spectra. Among our findings are included photoelectron spectral structure, different rates for different ionization channels, and several independent ATI series. All of these can be regarded as strong-field predictions for negative ions. Under the conditions studied, our results provide the first nonperturbative data on two-photon ionization pathways for the second electron. For reasons of computational

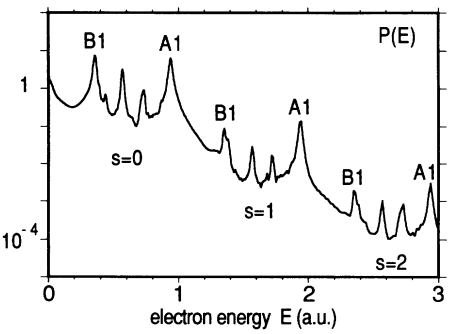

FIG. 4. Photospectrum $P(E)$ as in Fig. 2(b), displayed for energies from 0 to 3ω to show the distinct ATI series associated with each individual $s=0$ peak of Fig. 2(b).

efficiency, our study was one dimensional, but previous predictions based on 1D single-electron calculations [13] have been found to be in excellent qualitative agreement with both 3D calculations [14] and laboratory experiments, where they have existed. We expect that 1D calculations will also prove to be an efficient route to a satisfactory initial understanding of strong-field and nonperturbative two-electron physics.

We would like to acknowledge conversations with W. Becker, H. W. Bryant, P. H. Bucksbaum, T. F. Gallagher, and M. Halka as well as support from the National Science Foundation under PHY 88-22730 and PHY89-20108. In addition, R.G. acknowledges receipt of a Feodor Lynen Research Fellowship from the Alexander von Humboldt Foundation of Germany, as well as an NSF Research Associateship in Computational Science and Engineering. We also acknowledge grants for assistance with computing from the Pittsburgh Supercomputing Center and the Allied-Signal Corporation.

[1] See reviews in "Atoms in Intense Radiation Fields", edited by M. Gavrila (Academic, Orlando, to be published); and a large collection of papers in J. Opt. Soc. Am. B **7** (No. 4) (1990).

[2] P. Agostini, F. Fabre, G. Mainfray, G. Petite, and N. K. Rahman, Phys. Rev. Lett. **42**, 1127 (1979); see also the reviews, R. R. Freeman and P. H. Bucksbaum, J. Phys. B **24**, 325 (1991); and J. H. Eberly, J. Javanainen, and K. Rzążewski, Phys. Rep. **204**, 331 (1991).

[3] See, for example, G. Gibson, H. Jara, U. Johann, T. S. Luk, I. McIntyre, K. Boyer, and C. K. Rhodes, J. Opt. Soc. Am. B **4**, 595 (1987); X. F. Li, A. L'Huillier, M. Ferray, L. A. Lompre, and G. Mainfray, Phys. Rev. A **39**, 5751 (1989); as well as the reviews by A. L'Huillier and G. Mainfray and by C. K. Rhodes *et al.*, in Ref. [1].

[4] J. I. Gersten and M. H. Mittleman, J. Phys. B **9**, 2561 (1976); M. Gavrila and J. Kaminski, Phys. Rev. Lett. **52**, 613 (1984); see also reviews by J. H. Eberly *et al.*, M. Gavrila, and K. C. Kulander *et al.*, in Ref. [1].

[5] M. S. Pindzola, D. C. Griffin, and C. Bottcher, Phys. Rev. Lett. **66**, 2305 (1991).

[6] See J. Javanainen, J. H. Eberly, and Q. Su, Phys. Rev. A **38**, 3430 (1988); Q. Su and J. H. Eberly, Phys. Rev. A **44**, 5997 (1991). In the range of our present grid sizes ($\Delta x = 0.5$–1) the eigenvalues are only slightly different ($\pm 1\%$).

[7] The space coordinates have been discretized to a 1024×1024 lattice and the time-dependent Schrödinger equation has been solved with a split-operator fast-Fourier-transform method which has been discussed in detail in M. D. Feit, J. A. Fleck, Jr., and A. Steiger, J. Comput. Phys. **47**, 412 (1982).

[8] See, for example, the analysis of helium with the aid of rate equations by M. Crance and M. Aymar, J. Phys. (Paris) **46**, 1887 (1985); and the perturbative analyses by X. Tang and P. Lambropoulos, Phys. Rev. Lett. **58**, 108 (1987); and A. L'Huillier and G. Wendin, Phys. Rev. A **36**, 5632 (1987). For recent overviews of the status of negative ions and multielectron atoms in laser fields, see P. A. Golovinskii and I. Yu. Kiyan, Usp. Fiz. Nauk. **161**, 97 (1990) [Sov. Phys. Usp. **33**, 453 (1990)]; and C. A. Nicolaides, Th. Mercouris, and G. Aspromallis, J. Opt. Soc. Am. B **7**, 494 (1990).

[9] See W. W. Smith, C. Y. Tang, C. R. Quick, H. C. Bryant, P. G. Harris, A. H. Mohagheghi, J. B. Donahue, R. A. Reeder, H. Sharifian, J. E. Stewart, H. Toutounchi, S. Cohen, T. C. Altmann, and D. C. Rislove, J. Opt. Soc. Am. B **8**, 17 (1991); R. Trainham, G. D. Fletcher, N. B. Mansour, and D. J. Larson, Phys. Rev. Lett. **59**, 2291 (1987); R. R. Jones and P. H. Bucksbaum, Phys. Rev. Lett. **67**, 3215 (1991); and H. Stapelfeldt, D. G. Papaioannou, L. D. Noordam, and T. F. Gallagher, Phys. Rev. Lett. **67**, 3223 (1991).

[10] For descriptions of early work, see A. L'Huillier, L. A. Lompre, G. Mainfray, and C. Manus, Phys. Rev. A **27**, 2503 (1983); and T. S. Luk, U. Johann, H. Egger, H. Pummer, and C. K. Rhodes, Phys. Rev. A **32**, 214 (1985), and references therein.

[11] One study has reported many ATI series accompanying multiple-electron ionization: U. Johann, T. S. Luk, H. Egger, and C. K. Rhodes, Phys. Rev. A **34**, 1084 (1986).

[12] This pulse shape turns the field on as quickly as possible, consistent with drift- and displacement-free motion of a free electron in the same pulse. See R. Grobe, M. V. Fedorov, and J. H. Eberly (to be published).

[13] Our own work with the one-electron version of the present model has appeared, for example, in Ref. [6] as well as J. H. Eberly, Q. Su, and J. Javanainen, Phys. Rev. Lett. **62**, 881 (1989); Q. Su, J. H. Eberly, and J. Javanainen, Phys. Rev. Lett. **64**, 862 (1990); and R. Grobe and C. K. Law, Phys. Rev. A **44**, R4114 (1991). For other 1D calculations with the same model, see V. C. Reed and K. Burnett, Phys. Rev. A **42**, 3154 (1990); C. Cerjan, J. Opt. Soc. Am. B **7**, 680 (1990); J. Grochmalicki, M. Lewenstein, and K. Rzążewski, Phys. Rev. Lett. **66**, 1038 (1991); and V. C. Reed, P. L. Knight, and K. Burnett, Phys. Rev. Lett. **67**, 1415 (1991).

[14] See K. C. Kulander, K. J. Schafer, and J. L. Krause, in *Multiphoton Processes*, edited by G. Mainfray and P. Agostini (CEA Press, Paris, 1991), p. 119; and Phys. Rev. Lett. **66**, 2601 (1991).